

# Effect of Data Sources and DNI Effectiveness on CSP power plants Performances Assessment. Case Studies in Algeria.

Abdelkader ROUIBAH<sup>1\*</sup>, Chati TOUNSI<sup>2</sup>, Kamal MOHAMMEDI<sup>3</sup>, Kouider LAROUSSE<sup>1</sup>

<sup>1</sup> Laboratory Applied Automation and Industrial Diagnostics of University of Djelfa (LAADI), PO Box 3117, Djelfa 17000, Algeria; , E-mail: a.rouibah@univ-djelfa.dz

<sup>2</sup> Ziane Achour University of Djelfa 17000-Algeria

<sup>3</sup> URMPE, M. Bougara University, Boumerdès 35000-Algeria

\*Corresponding Author: Email a.rouibah@univ-djelfa.dz

## ARTICLE INFO

Received: 25 Dec 2024  
Revised: 21 Sep 2025  
Accepted: 29 Nov 2025

## ABSTRACT

This study presents a comparative assessment of high and medium resolution Direct Normal Irradiance (DNI) datasets, combined with real meteorological measurements and satellite-derived estimates, to evaluate their impact on the performance of Concentrated Solar Power (CSP) systems. The analysis focuses on four representative regions in Bechar, Elouad, Djelfa, and Biskra, and examines how the choice of DNI data source influences the resulting capacity factor (CF). The results show notable discrepancies across regions. In Bechar (DNI = 700 W/m<sup>2</sup>), a system with SM = 1.8 and 2 hours of TES generated 11.44 GWh/year with a CF of 6.7%. In Elouad (DNI = 750 W/m<sup>2</sup>), using SM = 1.2 and 2 hours of TES, annual production reached 7.4 GWh/year, corresponding to a CF of 4.2%. For Djelfa (DNI = 1050 W/m<sup>2</sup>), the same system with SM = 1.5 and 4 hours of TES achieved 18.45 GWh/year and a CF of 10.5%. Biskra exhibited the most striking contrast: with real DNI data (420 W/m<sup>2</sup>), SM = 1.3, and 6 hours of TES, the system delivered 71.51 GWh/year and a CF of 43.59%. When satellite-derived DNI was used instead, energy production increased to 75.7 GWh/year, raising the CF to 43.78%. These results highlight substantial performance variations driven by the choice of meteorological input data. The findings underscore the importance of selecting reliable DNI datasets for accurate CSP evaluation, ultimately supporting more effective system design, improved energy yield predictions, and the broader development of solar energy technologies in Algeria.

**Keywords:** DNI; Satellite-Derived Data; TMY; GHI; Concentrated Solar Power (CSP); Capacity Factor (CF); Solar Multiple (SM); Thermal Energy Storage (TES); Energy Efficiency.

## Introduction

The significance of DNI in optimizing solar energy systems is underscored by its critical role in electricity generation, particularly within concentrating solar power (CSP) systems. These systems rely on direct sunlight to convert solar energy into thermal energy, making DNI essential for their performance. Unlike other forms of solar radiation, DNI specifically measures the solar energy received by a surface directly oriented toward the sun. This concentrated sunlight is harnessed through mirrors or lenses, which transform it into heat energy used to drive turbines for electricity production. As global energy demands continue to rise, the precise measurement and understanding of DNI become increasingly vital for enhancing CSP technology and improving energy efficiency. By effectively capturing and utilizing DNI, solar power systems can significantly contribute to a sustainable and reliable energy future.

For instance, Philippe Blanc et al. delve into the intricacies of DNI by employing ISO standards and WMO guidelines, aiming to refine solar concentrator optimization. Their research addresses inconsistencies in DNI definitions and assesses the influence of circumsolar radiation, ultimately enhancing the performance evaluation of concentrating solar systems [1].

Similarly, Rouibah et al. analyze DNI's impact on solar tower power plant performance in Algeria, comparing real measurements with satellite data to reveal how local irradiance conditions affect energy output and efficiency. Their findings offer crucial insights for improving solar energy systems in comparable climatic regions [2]. Larbi Mohamed et al. focus on the Mechria region of Algeria, utilizing Sun Flux and SAM software to optimize the design of concentrated solar power plants through a detailed analysis of direct normal irradiance [3].

Oumaima et al. evaluated semi-empirical models for estimating DNI, finding the Kasten model most effective for optimizing active daylighting systems in Morocco's sunny climate [4]. Ailton Tavares et al. apply the Energy model to estimate hourly DNI from global horizontal irradiance and meteorological data, identifying potential Concentrating Solar Power sites and predicting annual DNI availability [5].

The Sandia National Laboratories' PV Performance Modeling Collaborative (PVPMC) focuses on enhancing the understanding and predictive accuracy of photovoltaic (PV) system performance. By providing comprehensive resources and methodologies, it promotes best practices within the solar industry, ultimately improving the reliability of performance models [6].

Moreover, Xie et al. present an algorithm of finite-surface integration to enhance DNI forecasting in cloudy conditions, particularly in the circumsolar region. This innovative approach aims to improve the reliability of solar energy models, benefiting photovoltaic system performance assessments [7]. A NASA Technical Report outlines a methodology for calculating monthly mean DNI and Global Tilted Irradiance (GTI) from (GHI) and (DHI) data, thus enhancing solar energy assessments and providing essential data for optimizing solar technology applications [8].

Zhang et al. evaluate methods for estimating DNI and GTI by deriving monthly averages from GHI and DHI, comparing two calculation approaches validated against BSRN and CERES data to offer insights for improving solar radiation models [9]. Lastly, Xie et al. apply a unique finite-surface integration method for calculating DNI under cloudy conditions, enhancing the accuracy of DNI measurements, which is critical for predicting solar resource availability [10].

This research presents a robust methodology that combines real-time meteorological data with satellite observations to analyze Direct Normal Irradiance levels. Leveraging the System Advisor Model, an advanced tool for solar energy analysis, the study conducts a detailed economic, technical, and thermal evaluation of a 20 MW solar power tower across different regions in Algeria. By examining critical parameters such as storage capacity and solar multiplicity, the research aims to optimize system design and reduce the levelized cost of electricity (LCOE). Various scenarios were explored, considering factors like annual energy production and operational costs, to provide actionable insights for enhancing the proficiency of solar energy systems in Algeria. Additionally, this study adopts a comprehensive framework to investigate the technical and thermal performance of the solar tower at four strategically selected sites in Algeria: Bechar, Eloued, Djelfa, and Biskra. A central focus is the assessment of DNI variability, which plays a pivotal role in determining the feasibility and performance of solar tower systems. Through SAM-based simulations, the research evaluates the operational characteristics and efficiency of the tower, offering valuable perspectives on its potential across Algeria's diverse climatic regions.

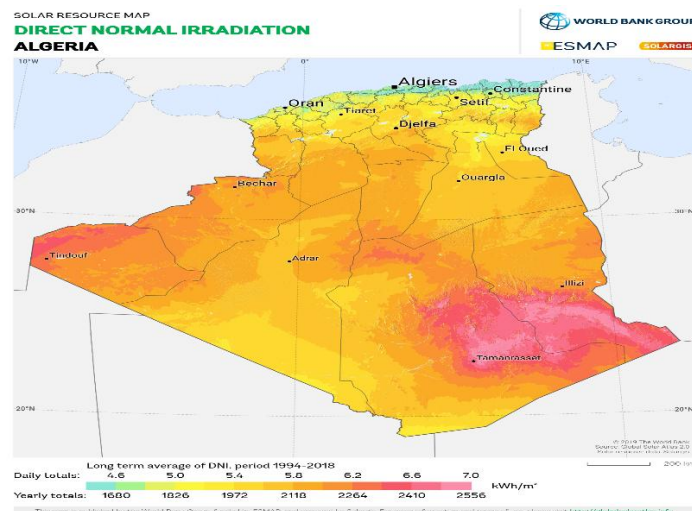


Fig. 1. The solar map illustrates the Direct Normal Irradiance (DNI) for the four stations analyzed.[28].

### Thermal Energy Storage

One of the standout benefits of using molten salt in CSP systems is the ability to store thermal energy. When sunlight is plentiful, any excess heat generated can be captured and stored in the molten salt. This allows the power plant to continue producing electricity even in cloudy weather or at night. This storage capability significantly boosts the reliability and flexibility of solar power, making it a strong competitor to traditional fossil fuel power plants [2,3,14,15,16,].

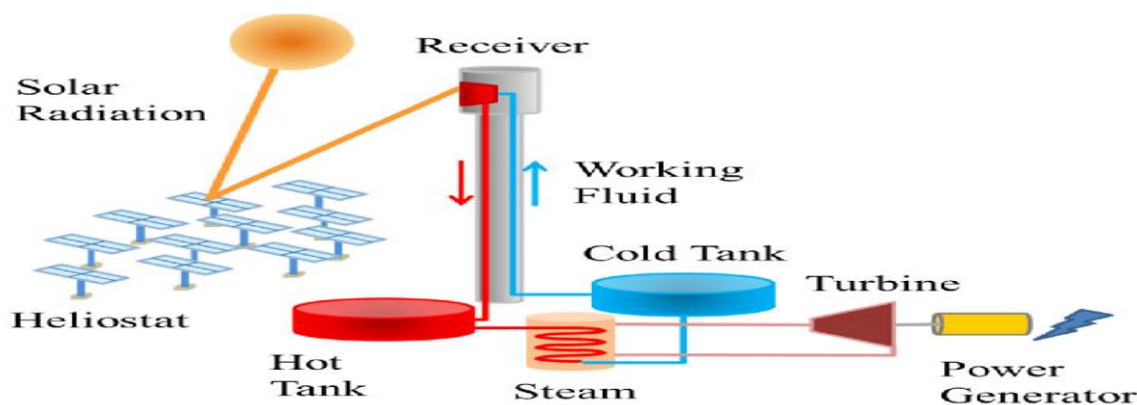


Fig. 2. Scheme of a Solar Tower Plant [25].

### Direct Normal Irradiance applications.

Precise measurements of Direct Normal Irradiance (DNI) are crucial for the design and optimization of solar energy systems, as they have a direct impact on the efficiency and output of Concentrating Solar Power (CSP) technologies. By understanding DNI levels, engineers can improve system performance and maximize energy production, ensuring that solar energy systems operate at their highest potential. [13]

### Direct Normal Irradiance types

Direct Normal Irradiance (DNI) can be categorized into several types based on specific conditions and measurement techniques.

#### 1.1. Satellite DNI (Remote Sensing Measurement)

Satellite-derived Direct Normal DNI uses satellite images and atmospheric models to estimate solar energy over large areas, providing valuable data in regions lacking ground measurements. Although less precise than ground-based measurements, improvements in satellite technology have increased the reliability of these estimates. [1].

### **1.2. Real DNI (Ground-Based Measurement)**

Real DNI measurements rely on ground-based devices, like pyrheliometers, which measure sunlight directly as it strikes a surface at a right angle. This method gives highly accurate data for a specific location, capturing the exact atmospheric influences present, including clouds, dust particles, and humidity. Such localized DNI data is often crucial for validating satellite estimates and provides accurate insights for assessing solar resources on a detailed, local level. However, these instruments can be costly and require maintenance, which makes continuous data collection challenging, particularly in remote or vast areas where equipment upkeep is not feasible. [5, 6]

### **1.3. Combined Approach (Real and Satellite DNI)**

Integrating real Direct Normal Irradiance (DNI) and satellite DNI data improves accuracy in solar energy applications by combining localized ground measurements with broad satellite coverage. This approach ensures a thorough assessment of solar resources, which is especially beneficial for planning large-scale solar projects that require both precise site data and extensive spatial insights.

## **Effectiveness of DNI**

- Maximum DNI represents the peak recorded value of DNI under ideal circumstances, typically observed during clear skies around solar noon when the sun is positioned at its zenith, with values potentially reaching up to  $1000 \text{ W/m}^2$  [1].
- Minimum DNI indicates the lowest recorded values, usually occurring during cloudy or overcast conditions, where atmospheric interference can cause significant reductions in direct sunlight [1].
- Medium DNI is an average calculated over a designated period, offering insights into typical DNI levels for a given location, which is essential for assessing solar energy potential [1].
- Calculate the optimal DNI from satellite filters DNI into intervals; every interval about  $200 \text{ W/m}^2$  beginning with intensities below  $200 \text{ W/m}^2$  and increasing to over  $1000 \text{ W/m}^2$ . For each range, the hours of direct radiation are counted, allowing for the selection of a design value from the range with the highest recorded hours. This approach helps optimize solar system performance by focusing on the most consistent radiation intensity for reliable energy generation [2].

## **Methodology**

This research adopts a thorough methodology to assess the technical and thermal performance of a 20 MW solar tower situated at four strategically chosen sites in Algeria: Bechar, Eloued, Djelfa and Biskra. We utilize the SAM, a well-regarded tool for solar energy system modeling, to simulate the operational features and efficiency of the solar tower. To elucidate the relationship between variations in Direct Normal Irradiance (DNI) and the efficiency of Concentrated Solar Power (CSP) systems, we correlated Capacity Factor (CF) with the Solar Multiple (SM). To achieve a comprehensive understanding, we integrated various data sources, including real-time weather observations and DNI measurements obtained from satellite imagery. We then conducted a comparative analysis to determine the accuracy and reliability of these data sources, examining their effects on the evaluation of solar energy systems across different geographic areas.

This methodology not only deepens our understanding of the role of DNI in CSP performance but also offers valuable insights for the design and optimization of solar installations in Algeria. The results of this analysis are anticipated to make a significant contribution to the development and implementation of solar technologies in the region.

To calculate DNI accurately, several fundamental formulas can be employed based on the relationship between Global Horizontal Irradiance (GHI), Diffuse Horizontal Irradiance (DHI), and other parameters. Here are the primary formulas used in DNI calculations:

- **Basic Relationship Between; GHI, DHI, and DNI [7]**

The fundamental equation relating. GHI, DHI and DNI Is:

$$GHI = DHI + DNI \cdot \cos(\theta_z) \quad (1)$$

Where:

$GHI$  = Global Horizontal Irradiance ( $W/m^2$ )

$DHI$  = Diffuse Horizontal Irradiance ( $W/m^2$ )

$\theta_z$  = Solar zenith angle (degrees)

From this equation, you can rearrange it to solve for DNI:

$$DNI = \frac{GHI - DHI}{\cos(\theta_z)} \quad (2)$$

- **DNI Calculation Using the Perez Model [7]**

The Perez model provides a method to estimate  $DNI$  based on  $GHI$  and  $DHI$ , Accounting for the solar position:

$DNI = \text{Function}(GHI, DHI, \text{solar position parameters})$

Where the function incorporates parameters like latitude, solar zenith angle, and azimuth.

- **Advanced Atmospheric Model for DNI [8]**

A more complex approach involves using atmospheric models to calculate DNI, which can be expressed as:

$$DNI = I_o \cdot m_a \cdot e^{-\delta R m_a} \quad (3)$$

Where:

$I_o$  = Solar constant (approximately  $1367 W/m^2$ )

$m_a$  = Optical air mass

$\delta R$  = Rayleigh optical thickness

- **Calculation from Sky Radiance Measurements [7]**

DNI can be computed from sky radiance measurements through integrals over specified solid angles, allowing for precise evaluations of solar energy distribution in various atmospheric conditions.

$$DNI = \frac{1}{A} \int_0^{2\pi} \int_0^\theta L(n, u) \sin(u) du d\theta \quad (4)$$

Where:

$L(n, u)$  = Sky radiance as a function of angle

$A$  = Area of the receiving surface

- **The GTI Isotropic Instantaneous Formula [8]**

$$I_T = (I - I_d) \left( \frac{\cos \theta}{\cos \beta} \right) + I_d \left( \frac{1 + \cos \beta}{2} \right) + I_{\rho_s} \left( \frac{1 - \cos \beta}{2} \right) \quad (5)$$

Where:

$I_T$  Is the hourly tilted, or total, irradiance on the tilted surface;

$\theta$  is the angle between the normal of the tilted surface and that of the beam sunlight;

$\beta$  is the tilt angle of the surface;

$I$  is the hourly GHI, and



$\rho_s$  is the monthly surface albedo.

The expression for  $\cos \theta$  is as follows:

$$\cos \theta = \cos Z \cos \beta + \sin Z \sin \beta \cos(\gamma_s - \gamma) \quad (6)$$

Where;

$\gamma_s$  is the azimuth angle of the Sun;

$\gamma$  is the azimuth angle of the tilted surface.

#### • Heliostat Field Efficiency Calculation [18]

Heliostat field efficiency  $\eta_h$  represents the proportion of solar energy reaching the receiver versus what the heliostat field intercepts, calculated by multiplying several efficiency factors.

$$\eta_h = \eta_{\cos} \cdot \eta_{att} \cdot \eta_{ref} \cdot \eta_{blk} \cdot \eta_{sha} \quad (7)$$

Where:

The heliostat field efficiency ( $\eta_h$ ) is determined by multiplying factors like cosine efficiency ( $\eta_{\cos}$ ), atmospheric attenuation efficiency ( $\eta_{att}$ ), reflection efficiency ( $\eta_{ref}$ ), blocking efficiency ( $\eta_{blk}$ ), and shading efficiency ( $\eta_{sha}$ ) each accounting for sunlight capture, reflection, and optimal heliostat positioning.

#### • Heliostat Field Layout Equation [19]

For the heliostat field layout, a common approach is to calculate the position and orientation of each heliostat to maximize energy capture. The radial staggered layout formula, for example, gives a basic arrangement:

$$R_i = R_{min} + \Delta R \times (i - 1) \quad (8)$$

Where:

$R_i$  : Radial distance of the  $i^{th}$  heliostat

$R_{min}$  : Minimum radial distance from the tower (dependent on tower height and field configuration)

$\Delta R$  : Distance increment calculated based on desired heliostat density, Fig.3.

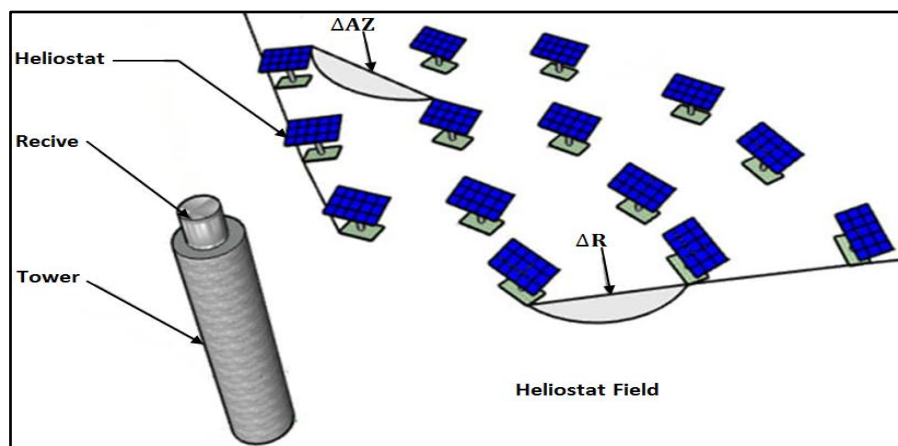


Fig. 3. Execution of the heliostats field.

#### • Cosine Efficiency [20]

Cosine efficiency ( $\eta_{\cos}$ ) is essential for determining how much sunlight each heliostat reflects toward the receiver, accounting for the angle of incidence:

$$\eta_{\cos} = \cos \theta \quad (9)$$

$\theta$ : Incidence angle between the sun's rays and the normal to the heliostat mirror surface, Fig.4.

This efficiency decreases as the angle between the heliostat and the sun deviates from  $90^\circ$ .

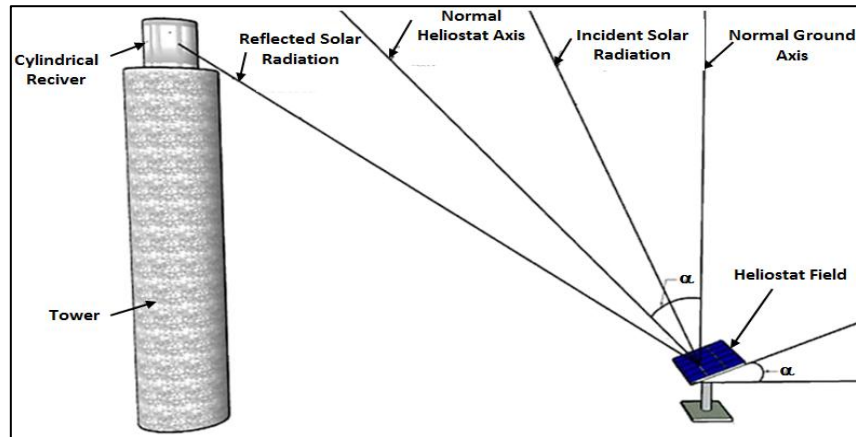


Fig. 4. Show cases the execution of the heliostats field, complete with a depiction of the optical angle  $\alpha$

- **Heat Transfer Rate (Q) [21]**

$$Q = \dot{m} \cdot Cp \cdot \Delta T \quad (10)$$

The heat transfer rate  $Q$  (in watts) is determined by the mass flow rate  $\dot{m}$  (in kg/s) of the molten salt, which represents how much salt circulates through the system. Additionally,  $Cp$  (in J/kg·°C) is the specific heat capacity of the molten salt, indicating the energy needed to raise the temperature of one kilogram of salt by one degree Celsius. The temperature difference  $\Delta T$  (in °C) reflects how much the salt's temperature increases as it absorbs heat from the solar receiver.

- **Energy Stored in the Molten Salt (E) [22]**

$$E = \dot{m} \cdot Cp \cdot (T_{out} - T_{in}) \quad (11)$$

The total energy  $E$  stored in the molten salt (in joules) is calculated using the mass flow rate  $\dot{m}$  (in kg/s) and the specific heat capacity  $Cp$  (in J/kg·°C). The difference between the outlet temperature  $T_{out}$  and the inlet temperature  $T_{in}$  indicates the amount of heat energy stored in the molten salt.

- **Heat Losses [23]**

The heat loss  $Q_{Loss}$  from the system is calculated using the equation:

$$Q_{Loss} = U \cdot A \cdot (T_{av} - T_{am}) \quad (12)$$

Where  $U$  represents the overall heat transfer coefficient (W/m<sup>2</sup>·°C),  $A$  is the surface area (m<sup>2</sup>) from which heat is lost,  $T_{av}$  is the average temperature of the molten salt (°C), and  $T_{am}$  is the ambient temperature (°C), indicating that the difference  $(T_{av} - T_{am})$  serves as the driving force for heat loss.

- **Efficiency of the Receiver [24]**

$$\eta_{receiver} = \frac{Q}{Q_{solar}} \quad (13)$$

$\eta_{receiver}$ : Is the efficiency of the solar receiver, indicating how effectively it converts solar energy into usable heat.

$Q$ : is the heat absorbed by the molten salt (W).

$Q_{solar}$ : represents the solar energy incident on the receiver (W). This equation provides a measure of how much of the incoming solar energy is converted into thermal energy.

- **Solar Multiple (SM) [22]**

Solar Multiple reflects the ratio of solar energy received by the receiver to the thermal energy required for the power generation process.

$$SM = \frac{Q_{solar}}{Q_{thermal}} \quad (14)$$

The total solar energy incident on the receiver denoted as  $Q_{\text{solar}}$  (in watts), is influenced by factors such as solar irradiance and the size of the heliostat field, while  $Q_{\text{thermal}}$  represents the thermal energy required to generate electricity (in watts) at the power block's rated capacity.

A higher SM indicates that the CSP system can produce more thermal energy than the minimum needed, enhancing energy efficiency during peak sunlight hours.

#### • Capacity Factor (CF) [25]

The Capacity Factor measures the actual Annual Energy of the CSP power tower relative to its maximum potential output.

$$CF = \frac{E_{\text{actual}}}{E_{\text{Max}}} \quad (15)$$

The actual energy produced by the CSP plant over a specified period is referred to as  $E_{\text{actual}}$  (in KWh), indicates the plant's performance, while  $E_{\text{Max}}$  represents the maximum energy that could be generated if the plant operated at full capacity continuously during that same period (in KWh).

Capacity Factor (CF) is critical in evaluating the reliability and operational performance of the power tower system, with higher values indicating better utilization of the plant's installed capacity.

#### • Thermal Energy Storage (TES) [26]

Thermal Energy Storage (TES) represents the total thermal energy stored in the molten salt or heat transfer fluid within the CSP system (J).

$$TES = \dot{m} \cdot C_p \cdot (T_{\text{max}} - T_{\text{min}}) \quad (16)$$

The mass flow rate of the heat transfer fluid, denoted as  $\dot{m}$  (in kg/s), combined with its specific heat capacity  $C_p$  (typically ranging from 1.5 to 2.0 kJ/kg.°C for molten salt) and the maximum  $T_{\text{max}}$  and minimum  $T_{\text{min}}$  temperatures during operation (in °C), illustrates the energy that can be stored based on the fluid's flow rate and temperature difference. By storing thermal energy, CSP plants with power tower configurations can continue to generate electricity during non-sunny periods, enhancing grid stability and energy reliability.

This methodology lays a solid foundation for evaluating the performance of a 20 MW solar tower across various regions in Algeria. By combining different data sources and conducting a comparative analysis of DNI, we aim to strengthen the credibility of our findings. Our exploration of the connection between DNI levels and the CF is intended to provide essential insights into the efficiency of concentrated solar power systems.

Ultimately, the rigor of this study's methodology not only deepens our understanding of solar energy dynamics but also offers practical design insights for future solar installations in Algeria. Through these initiatives, we hope to contribute to the growth of solar technologies and support the development of sustainable energy solutions in the region.

## Results and discussion

In this section, we will share the insights gained from our analysis of the 20 MW Solar Tower across four locations in Algeria: Bechar, Eloued, Djelfa, and Biskra. We will explore how DNI measurements gathered from both real weather data and satellite sources impact the CF and SM of the CSP system. These findings will provide a clearer picture of the solar tower's operational efficiency under different climatic conditions. Additionally, we will discuss the significance of these results for the design and optimization of solar installations in Algeria. Ultimately, this section highlights the crucial role that accurate DNI assessment plays in enhancing the feasibility of solar energy projects in the region.

### 1.4. Region of Biskra

Figure (5) shows the impact of Thermal Energy Storage (TES) on annual energy production per square meter of heliostats with different Solar Multiple (SM) values, indicating that higher SM generally leads to increased energy output. However, this enhancement shows diminishing returns as TES levels rise, primarily due to inefficiencies in



energy retrieval linked to larger storage capacities. An optimal performance balance is achieved with moderate SM values between 1.2 and 1.5 and TES levels of 4 to 6 hours, effectively capturing solar energy while reducing the drawbacks of extensive storage systems. For instance, an SM of 1.3 with a TES of 6 hours yields approximately 375.24 kWh/m<sup>2</sup> (75.7 GWh), illustrating its effectiveness in areas with variable sunlight. These findings underscore the importance of strategically optimizing both SM and TES to enhance the overall efficiency and viability of concentrated solar power (CSP) systems.

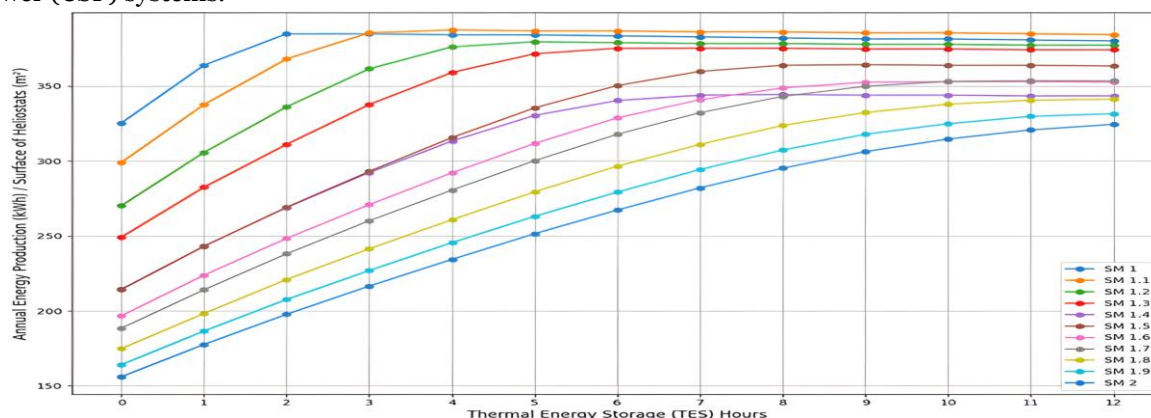


Fig. 5. The impact of Thermal Energy Storage (TES) on annual energy production per square meter of heliostats with different Solar Multiple (SM) values,

Figure (6) presented Solar multiple (SM) effect on Annual Energy production (kwh) /surface of heliostats under different TES values. It indicates that an increase in the Solar Multiple (SM) generally correlates with enhanced annual energy output per square meter of heliostats. However, this improvement exhibits diminishing returns as the level of Thermal Energy Storage (TES) rises, attributable to inefficiencies in energy retrieval linked to higher storage capacities. It is essential to achieve a balance between SM and TES for optimal performance; specifically, a moderate SM in the range of 1.2 to 1.5, coupled with a TES level of 4 to 6, effectively captures solar energy while mitigating the inefficiencies associated with larger storage systems. For instance, at an SM of 1.3 and a TES of 6, the configuration achieves an annual energy production of approximately 375.24 kWh/m<sup>2</sup>, demonstrating suitability for regions with variable sunlight by maximizing energy generation while minimizing reliance on costly storage solutions.

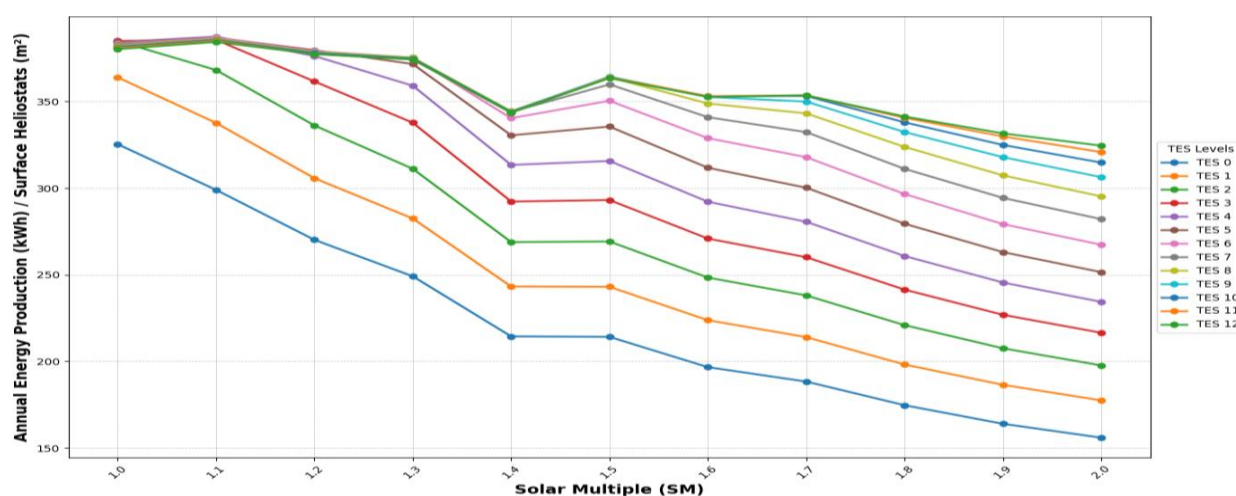


Fig. 6. Solar multiple (SM) effect on Annual Energy production (kwh)/surface of heliostats under different TES values.

The figure (7) clearly illustrates the multiple solar effects on capacity factors under different TES values, emphasizing the crucial role of solar multiples in enhancing performance. As TES hours increase from 0 to 2, we observe a notable improvement in capacity factors, peaking at around 59% for higher solar multiples (1.1 to 1.9). When we focus on the capacity factor from 2 to 6 hours of TES, a consistent upward trend becomes evident, particularly for solar multiples 1.2 and 1.4. For solar multiple 1.2, the capacity factor rises from 36.0394% at 2 hours to 48.7037% at 6 hours, showing an increase of 12.6643%. Meanwhile, solar multiple 1.3 demonstrates a more pronounced rise, with the capacity factor going from 36.3% at 2 hours to 43.78% at 6 hours. These findings underscore the significance of integrating longer TES durations with optimal solar multiples, as this combination enhances CSP efficiency and reinforces the potential of solar energy as a practical and sustainable power source in regions abundant in solar resources, such as Algeria.

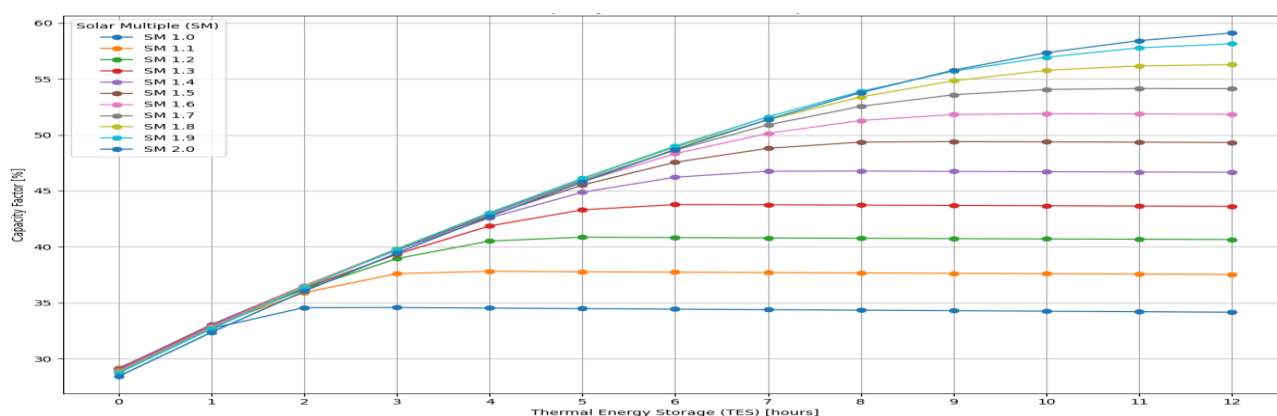


Fig. 7. The Thermal Energy Storage effect on capacity factors under different SM values

### 1.5. The four regions: Bechar, Elouad, Djelfa and Biskra

In Figure (8); we can observe the electricity production per square meter for the four regions, with the SM values given in two diverse groups of curves. For the regions of Bechar and Elouad, the curves' evolution is coherent and remarkably close to each other. This is because the simulation was based on real meteorological data and the high efficiency of the Direct Normal Irradiance (DNI).

The curves of the Djelfa and Biskra regions have different trajectories. This dissimilarity is the result of the use of divergent methodologies in the simulation process. In particular, the Djelfa region used meteorological data derived from satellites and improved the efficiency of direct normal irradiance (DNI), while the Biskra region used real meteorological data and achieved moderate DNI efficiency.

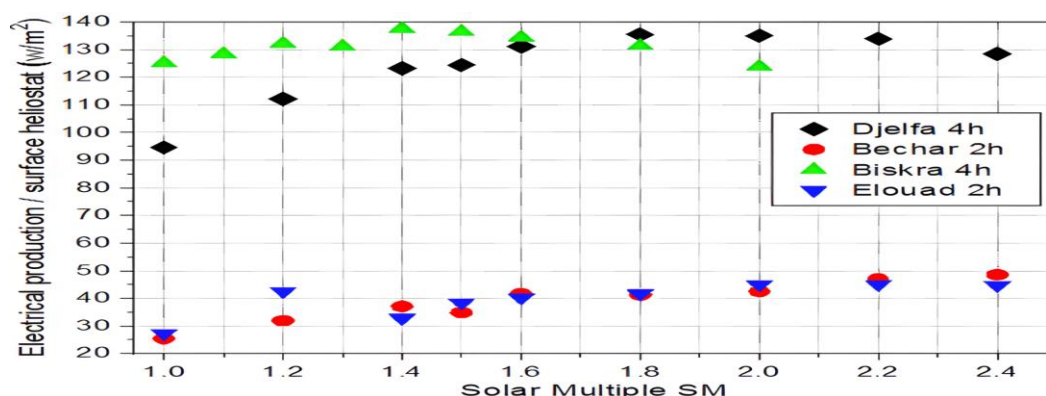


Fig. 8. Evolution of electricity production per heliostat area as a function of the solar multiple effect in the four regions (Bechar, Elouad, Djelfa, Biskra).

In Figure (9), the capacity factor (CF) evolves proportionally with the Solar Multiple (SM), and the curves increase proportionally while deviating irregularly and gradually. This is due to the influence of the effectiveness of Direct Normal Irradiance (DNI):

- For the Djelfa region, we have a high direct normal irradiation from satellite data.
- For the Biskra region, we observe average direct normal irradiation based on real weather data.
- For the regions of Bechar and Elouad, direct normal irradiation is high and based on real weather observations.

From the above, we can conclude that the results obtained from satellite weather data are very significant, as are the actual results when the efficiency of DNI is high. On the other hand, the results obtained from the actual data, but with an average efficiency of the DNI, stand out clearly among all the results.

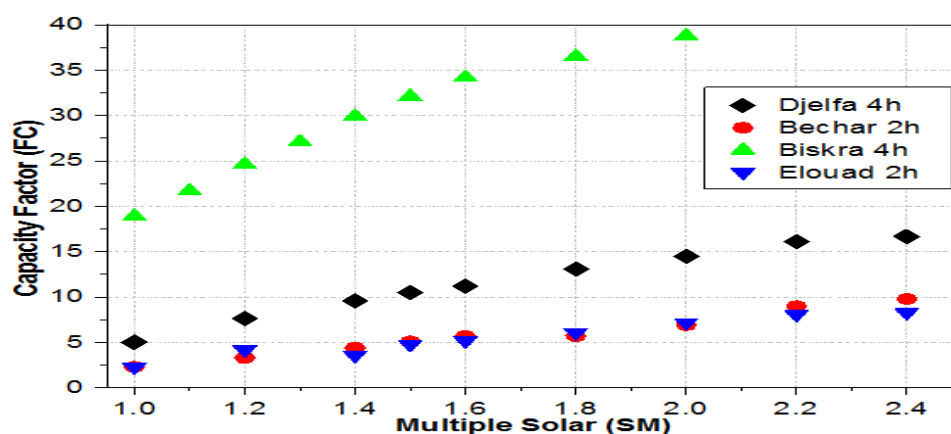


Fig. 9. Solar Multiple effect on the Capacity Factor (CF) of the different regions (Bechar, Elouad, Djelfa and Biskra).

### 1.6. Comparison

Table 1 shows a comparison between the annual energy production values and the power factor for the four different regions.

Table 1. Comparison between the annual energy production values and the Capacity factor for the different regions

Regions	DNI (W/M <sup>2</sup> )	SM	TES	Annual Energy production (Gwh)	Capacity Factor (%)	data
Bechar	700 (élevé)	1.8	2h	11.44	6.7	Real
Eloued	750 (élevé)	1.2	2h	7.4	4.2	Real
Djelfa	1050	1.5	4h	18.45	10.5	Satellite
Biskra (our study)	708 (effective)	1.3	6h	75.7	43.78	Satellite

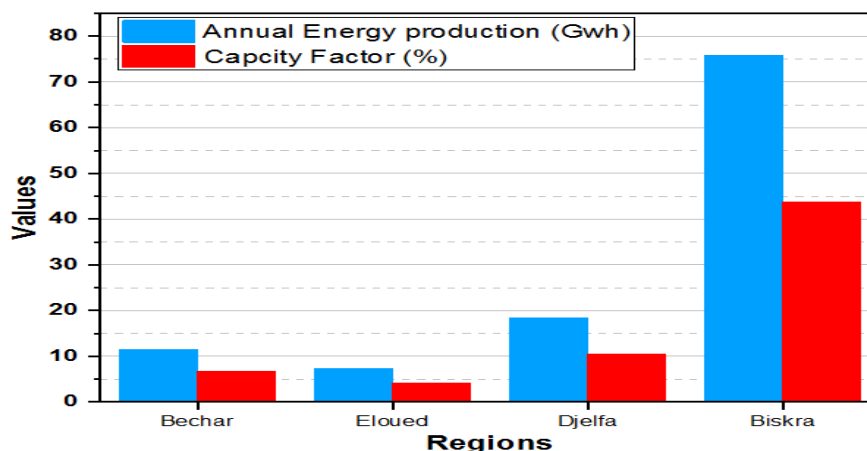


Fig. 10. Comparison of Annual Energy Production and Capacity Factor for Different Regions.

The figure (10) presents a comparative analysis of annual energy production and capacity factor across various regions, highlighting the significant impact of solar resource availability, Solar Multiple (SM), and Thermal Energy Storage (TES) on Concentrated Solar Power (CSP) system performance. Biskra Region (our study) moderate DNI of  $708 \text{ W/m}^2$  and optimal TES durations (6 hours), demonstrate the highest capacity factor (43.78%) and substantial energy production (75.7 GWh). In contrast, regions with lower Solar Multiple values and shorter Thermal Energy Storage durations, such as Eloued ( $750 \text{ W/m}^2$ , 2 hours of TES), show significantly lower capacity factors (4.2%) and energy production (7.4 GWh). These findings emphasize the importance of combining high DNI, extended TES, and optimal SM in maximizing CSP efficiency and output. The correlation between capacity factor and energy production underscores the potential of CSP systems in regions with favorable solar conditions, such as Algeria, where such configurations can significantly contribute to sustainable energy generation.

## Conclusion

This study demonstrates the essential influence of Direct Normal Irradiance (DNI) data, whether obtained from ground-based measurements or satellite-derived sources, on the evaluation and optimization of Concentrated Solar Power (CSP) systems in Algeria. By examining four distinct regions (Bechar, Elouad, Djelfa, and Biskra), the analysis provides valuable insight into how the choice of DNI dataset affects energy production and overall system performance.

In Bechar ( $\text{DNI} = 700 \text{ W/m}^2$ ), a system configured with a Solar Multiple (SM) of 1.8 and 2 hours of Thermal Energy Storage (TES) produced 11.44 GWh annually, corresponding to a capacity factor (CF) of 6.7%. For Elouad ( $\text{DNI} = 750 \text{ W/m}^2$ ), using  $\text{SM} = 1.2$  and 2 hours of TES, annual production reached 7.4 GWh with a CF of 4.2%. In Djelfa ( $\text{DNI} = 1050 \text{ W/m}^2$ ), an SM of 1.5 paired with 4 hours of TES resulted in 18.45 GWh/year and a CF of 10.5%.

Biskra presented the most pronounced variability. Using real measured DNI values ( $420 \text{ W/m}^2$ ), the system with  $\text{SM} = 1.3$  and 6 hours of TES generated 71.51 GWh/year with a CF of 43.59%. When satellite-derived DNI data ( $708 \text{ W/m}^2$ ) was used for the same configuration, production increased to 75.7 GWh/year, and the CF improved to 43.78%.

The correlation analysis between capacity factor, solar multiple, and DNI highlights the importance of selecting accurate solar resource data when designing CSP systems. The findings suggest that integrating high-quality satellite-derived DNI datasets can enhance performance estimates, improve system sizing, and support the broader deployment of efficient and resilient solar energy technologies in Algeria.

## Further Research

- By comparing the CSP plant configurations that deliver the best performance, it becomes clear that thermal storage systems are essential for increasing the competitiveness of CSP technology. Their integration allows CSP to compete with, and complement, other existing energy sources by improving performance predictability, lowering overall costs, and offering greater flexibility in electricity dispatch.
- The main design parameters of these plants, such as the design-point DNI, the solar multiple, and the number of thermal storage hours, were determined with the objective of achieving the lowest possible levelized cost of energy (LCOE).

## References

- [1] Cameron, I., & Sinha, A. (2012). Direct normal irradiance related definitions and applications: The circumsolar issue. *Solar Energy*, 86(8), 2261-2272.
- [2] Rouibah, A., Benazzouz, D., Kouzou, A. L., & Hafaifa, A. (2020). The Impact of Direct Normal Irradiation on the Solar Tower Power Plant Performance based on Real and Satellite Data: Analysis on Algerian Regions. *Electrotehnica, Electronica, Automatica*, 68(2), 60-72.
- [3] Larbi, M., Rouibah, A., Guemana, M., & Laissaoui, M. (2023). An analytical study of direct normal irradiance for concentrated solar energy applications for the Mechria region of Algeria. *International Conference on Applied Engineering and Natural Sciences*, 1(1), 565-569.
- [4] Oumaima, H., Oukali, A., & El Boujaady, H. (2021). Evaluation of semi-empirical models for estimating direct normal irradiation: A case study for active daylighting systems in Morocco. *Renewable Energy*, 169, 234-241. <https://doi.org/10.1016/j.renene.2021.01.021>
- [5] Tavares, A., Da Silva, F. M., & De Oliveira, A. D. (2020). Application of the Engerer model for estimating hourly direct normal irradiance from global horizontal irradiance and meteorological data: Identifying potential concentrating solar power sites. *Renewable Energy*, 147, 1442-1450. <https://doi.org/10.1016/j.renene.2019.08.076>
- [6] Sandia National Laboratories. (2024). PV performance modeling collaborative (PVPMC). Retrieved from <https://pvpmc.sandia.gov/>
- [7] Xie, Y., Sengupta, M., Liu, Y., Long, H., Min, Q., & Liu, W. (2020). A novel finite-surface integration algorithm for forecasting direct normal irradiance (DNI) in cloudy conditions.
- [8] National Aeronautics and Space Administration. (2024). Calculating monthly mean direct normal irradiance (DNI) and global tilted irradiance (GTI) from GHI and DHI data. NASA Technical Report..
- [9] Zhang, T., Stackhouse, P. W., Jr., Macpherson, B., & Mikovitz, J. C. (2023). Monthly mean DNI and GTI derived from monthly mean GHI and DHI.
- [10] Solar PACES. (2018). How CSP works: Tower, trough, Fresnel or dish. Retrieved October 29, 2024, from <https://www.solarpaces.org/how-csp-works-tower-trough-fresnel-or-dish/>
- [11] Wikipedia. (2023). Solar power tower. Retrieved October 26, 2024, from [https://en.wikipedia.org/wiki/Solar\\_power\\_tower](https://en.wikipedia.org/wiki/Solar_power_tower)
- [12] Argonne National Laboratory. (2024). Concentrating solar power (CSP) technologies. Retrieved October 29, 2024, from <https://www.anl.gov/article/concentrating-solar-power-csp-technologies>
- [13] Solar PACES. (2024). How concentrated solar power works. Retrieved October 26, 2024, from <https://www.solarpaces.org/how-concentrated-solar-power-works/>
- [14] Crawley, D. B., & Lawrie, L. K. (2015, December). Rethinking the TMY: is the 'typical' meteorological year best for building performance simulation. In *Conference: Building Simulation* (pp. 2655-2662).
- [15] Collado, F., & Tellez, F. (1990). Calculation of the annual energy from central receiver solar power plants. *Solar Energy*, 45(4), 191-199.
- [16] Sánchez, M., & Romero, M. (2006). Methodology for generation of heliostat field layout in central receiver systems based on yearly normalized energy surfaces. *Solar Energy*, 80(7), 861-874.



- [17] Zhu, G., Neises, T., & Ho, C. K. (2014). Heliostat canting and focusing to maximize annual performance of a solar tower plant. *Solar Energy*, 103, 227-237.
- [18] Duffie, J. A., & Beckman, W. A. (2013). *Solar engineering of thermal processes* (4th ed.). Wiley.
- [19] Kearney, D. (2009). *Concentrating Solar Power Technology*. Solar Energy Research Institute.
- [20] Gokhale, A. A., & M. V. (2017). Thermal Performance of Molten Salt in Solar Thermal Power Plants. *Renewable and Sustainable Energy Reviews*.
- [21] Behar, O., & S. A. (2021). Performance Evaluation of Concentrated Solar Power (CSP) Systems. *Journal of Solar Energy Engineering*.
- [22] Turchi, C. (2010). *Concentrating Solar Power Projects in the United States*. National Renewable Energy Laboratory.
- [23] Dersch, J., & W. D. (2012). Thermal Energy Storage for Solar Power Plants. *Solar Energy*.
- [24] System Advisor Model (SAM). (2021, December 2). SAM: The System Advisor Model. National Renewable Energy Laboratory.
- [25] Nouri, M., Chaker, A., Behar, O., & Yaiche, M. R. (2013). Scheme of a solar tower plant [Figure]. In *Study of the influence of meteorological parameters on the performance of a solar power tower plant in Algeria*. ResearchGate Kearney, D. (2009). *Concentrating Solar Power Technology*. Solar Energy Research Institute..
- [26] Schreck, S., Schroedter-Homscheidt, M., Klein, M., & Cao, K.-K. (2020). Satellite image-based generation of high frequency solar radiation time series for the assessment of solar energy systems. *Meteorologische Zeitschrift*, 29(3), 397–410.
- [27] Lara-Fanego, V., Gutiérrez, J., & Rodríguez, M. (2012). Evaluation of the WRF model solar irradiance forecasts in Andalusia (southern Spain). *Solar Energy*, 86(8), 2200-2217.
- [28] Solar GIS. (2024). Solar irradiation data. Retrieved from <http://solargis.info/doc/free-solar-radiation-maps-DNI>.